An automated method for detecting architectural distortions on mammograms using direction analysis of linear structures*

T. Matsubara, A. Ito, A. Tsunomori, T. Hara, C. Muramatsu
T. Endo and H. Fujita

Abstract—**Architectural distortion is one of the most important findings when evaluating mammograms for breast cancer. Abnormal breast architecture is characterized by the presence of spicules, which are distorted mammary structures that are not accompanied by an increased density or mass. We have been developing an automated method for detecting spiculated architectural distortions by analyzing linear structures extracted by normal curvature. However, some structures that are possibly related to distorted areas are not extracted using this method. The purpose of this study was to develop a new automated method for direction analysis of linear structures to improve detection performance in mammography. The direction of linear structures in each region of interest (ROI) was first determined using a direction filter and a background filter that can define one of eight directions (0°, 22.5°, 45°, 67.5°, 90°, 112.5°, 135°, and 157.5°). The concentration and isotropic indexes were calculated using the determined direction of the linear structures in order to extract the candidate areas. Discriminant analysis was performed to eliminate false positives results. Our database consisted of 168 abnormal images containing 174 distorted areas and 580 normal images. The sensitivity of the new method was 81%. There were 2.6 and 4.2 false positives per image using the new and previous methods, respectively. These findings show that our new method is effective for detecting spiculated architectural distortions.**

I. Introduction

Mammography is the most effective screening tool available for early detection of breast cancer. Clustered microcalcifications, masses, and architectural distortions are significant findings when interpreting mammograms for the presence of breast cancer.

The structure of the breast is loosely arranged along duct lines. In a normal breast image, these ducts are directed towards the nipple. Cancer is suspected on mammograms with architectural distortions in which the orientation of these structures deviates towards a point [1]. However, architectural distortions frequently have a subtle appearance on mammograms, making them difficult to diagnose for physicians [2, 3]. Previous mammography computer-aided diagnosis (CAD) studies have focused on either clustered microcalcifications or masses or both. Baker et al. reported that the sensitivities of two commercially available computer-aided detection (CADe) systems for detecting architectural distortions were as low as 21% to 38% [4]. There is a need for a CADe system that is specialized in the detection of architectural distortions.

Several groups have reported techniques for detecting architectural distortions. Karssemeijer et al. proposed a method based on the statistical analysis of a map of pixel orientations for detecting stellate patterns [5]. Approximately 90% of the malignant cases were detected with a rate of one false positive (FP) per image. Guo et al. investigated a support vector machine for the detection of architectural distortions in mammographic images by employing the Hausdorff dimension concept [6]. The dataset used in this investigation contained 19 regions of interest (ROIs) with architectural distortions and 21 ROIs with normal patterns from the Mammographic Image Analysis Society (MIAS) database. An accuracy of 72.5% was achieved in classifying normal patterns versus architectural distortions in ROIs. Tourassi et al. explored the use of the fractal dimension to differentiate between normal and architectural distortion patterns in mammographic ROIs that were selected from the Digital Database for Screening Mammography (DDSM) [7]. This study was performed using 112 ROIs with architectural distortions and 1,388 normal ROIs. The area under the receiver operating characteristic (ROC) curve was 0.89. The authors also showed that the average fractal dimension of the normal ROIs was significantly higher than that of the ROIs that had architectural distortions. Rangayyan et al. used Gabor filters and measures of the divergence of oriented patterns for the detection of architectural distortions on mammograms [8]. The proposed method was applied to 106 prior mammograms before clinical diagnosis of breast cancer from 56 interval-cancer patients and 52 mammograms from 13 normal patients. The area under the ROC curve was 0.75. Yoshikawa et al. proposed an automated architectural distortion detection method using an improved adaptive Gabor filter, which consisted of three Gabor filters created by changing the combination of parameters [9]. This technique was evaluated using 50 mammograms. The authors reported that the true positive (TP) rate was 82.45%, and the number of FPs per image was 1.06.

We have been developing an automated method for detecting spiculated architectural distortions by analyzing linear structures extracted by normal curvature [10].

*Research supported by a Grant-in-Aid for Scientific Research on Innovative Areas (26108005), MEXT, Japan.

T. Matsubara is with Nagoya Bunri University, Aichi, JAPAN (phone: +81-587-23-2400; fax: +81-587-21-2844; e-mail: matsubara.tomoko@nagoya-bunri.ac.jp).

A. Ito, T. Hara, C. Muramatsu and H. Fujita are with Gifu University, Gifu, JAPAN (e-mail: {aito, hara, chisa, fujita}@fjt.info.gifu-u.ac.jp).

A. Tsunomori is with KONICA MINOLTA,Inc, Tokyo, JAPAN (e-mail: akinori.tsunomori@konicaminolta.com)

T. Endo is with National Hospital Organization East Nagoya Hospital, Aichi, JAPAN (e-mail: endot@hosp.go.jp)

978-1-4244-9270-1/15/$31.00 ©2015 IEEE

However, some structures that are possibly related to distorted areas are not extracted by this method. The purpose of this study was to develop a new automated method for direction analysis of linear structures in order to improve the detection performance in mammography.

II. METHODS

Approval for the study was obtained from the ethics boards of Nagoya Bunri University and Gifu University.

A flowchart of our previous and new methods for the extraction of spiculated architectural distortions is shown in Fig. 1. Details of the techniques are described below.

A. Limitations using the previous method

Our previous method consisted of three steps: i) extraction of linear structures by normal curvature, ii) extraction of candidate areas by concentration and isotropic indexes, iii) elimination of FPs. In step i), first, a 3-D space where the z-axis is the density (pixel value) of the 2-D mammogram was created. In this 3-D representation, dense linear structures have low values and fatty regions have high values. The linear structure in the mammary gland is described by a downward-curved surface. Secondly, the distribution of density is approximated on a curved surface in order to calculate the normal curvature. Based on visual assessment, it was clear that some linear structures with a background trend were not adequately approximated under the influence of the background. Figure 2 illustrates this problem. Therefore, the current normal curvature of the linear structures with a background trend was not calculated and the linear structures were not extracted. It is necessary to extract linear structures without background influence.

B. Extraction of linear structure using linear direction analysis

Using our new method, the linear structures are extracted using the direction and background filters. Figure 3 shows the eight direction filters (0°, 22.5°, 45°, 67.5°, 90°, 112.5°, 135°, and 157.5°) and eight background filters.

The breast region is first divided into ROIs. The size of each ROI is 9 pixels * 9 pixels (1.8 mm * 1.8 mm). Second, the eight direction filters and eight background filters in each ROI are calculated. If the output value calculated by either of the direction filters is smallest, the direction of the ROI is defined as the one that the filter shows. If the output value calculated by either of the background filters is smallest, by definition

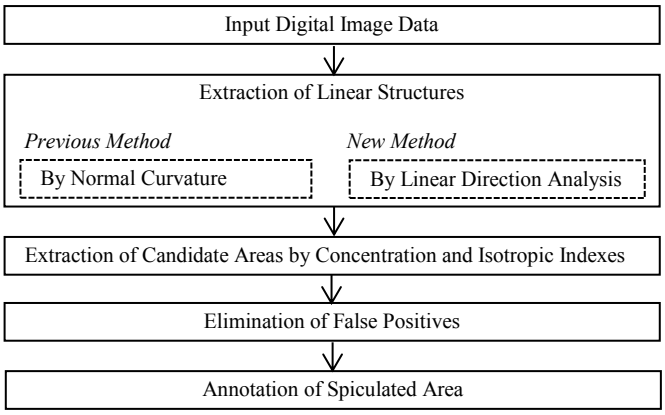

Figure 1. Flowchart of our previous and new methods for the extraction of spiculated architectural distortions.

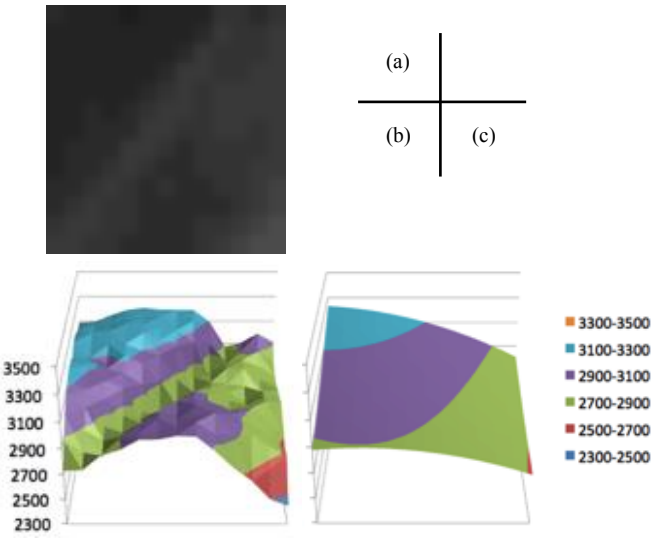

Figure 2. Limitations of our previous method.
(a) Region of interest (ROI) having linear structures on background trends in the original image. (b) 3-D space where the z-axis is the density (pixel value) of (a) in a 2-D mammogram. (c) Approximated curved surface in (b). The linear structure is lost because the density change of the background trend is large compared to one of linear structure.

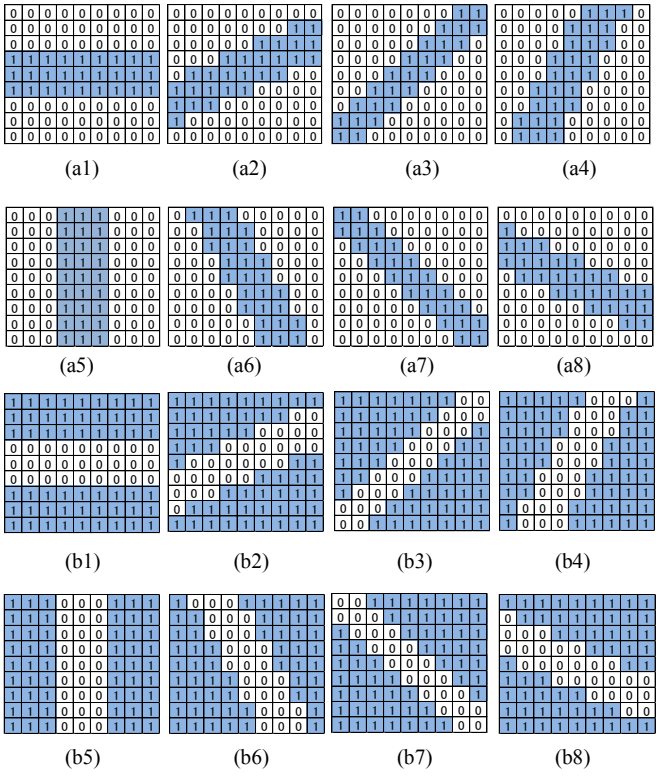

Figure 3. Eight direction filters (a1-a8) and eight background filters (b1-b8).

there is no direction in that ROI. By using this technique, the calculated output value in Figure 2 (a) and the direction filter (a3) is the smallest. Therefore, it is possible to define the correct direction of Figure 2 (a), as 45 degrees. Figure 4 and 5 show examples of ROIs with and without linear structures and examples of linear structures extracted by the new method, respectively.

C. Extraction of candidate areas using concentration and isotropic indexes

The concentration index represents the degree of concentration of linear structures. This index is high in the distorted areas, because the linear structures of the mammary gland are toward the suspect area. However, the concentration indexes are high not only in the distorted area but also in linear structures, such as blood vessels. The isotropic index of the distorted areas is high, whereas that of blood vessels is low. Through the use of isotropic indexes, it is possible to discriminate between distorted areas and blood vessels. Therefore, the candidate areas are extracted using both concentration and isotropic indexes.

D. Elimination of false positives

First, the candidate, that corresponds to the outlier (defined by a small size or high mean pixel value) is eliminated in order to improve performance of the following discriminant analysis. Nine features are employed in discriminant analysis. When the distorted and normal regions are compared, the distorted mammary gland tissue tends to appear in light areas, whereas the regions surrounding architectural distortions tend to be dark because those areas contain a large amount of fat tissue. The contrast between the suspect area and the surrounding area is high. Five features, the size, the mean pixel value, the mean concentration index, the mean isotropic index, and the contrast between the suspect area and its surroundings, are calculated in the suspect area. The intensity variation of the power spectra of the typical FP area is more evident than that of the typical TP area. TP areas have a symmetrical profile and FP areas have asymmetrical profile. Four features, the root-mean-square variation, the first moment, the difference of averages profiles, and the difference of the slope magnitude of linearization of profiles, are calculated in power spectrum. These nine features are selected and the round robin method is used to estimate the performance.

The residual candidates are annotated as spiculated architectural distortions.

III. Results and Discussion

Our database consisted of 168 abnormal images that contained 174 distorted areas and 580 normal images. Figure 6 shows the free-response receiver operating characteristic (FROC) curves using our previous and new methods. At the first pick-up stage, the previous method yielded a maximum of 163 TP areas, while the new method yielded 168. The sensitivity was 94% and 97% with 17.0 and 17.2 FPs per image using the previous and new methods, respectively. These curves show that the new method results in higher performance. In particular, at the same sensitivity of 81%, the numbers of FPs per image were 4.2 and 2.6 in the previous

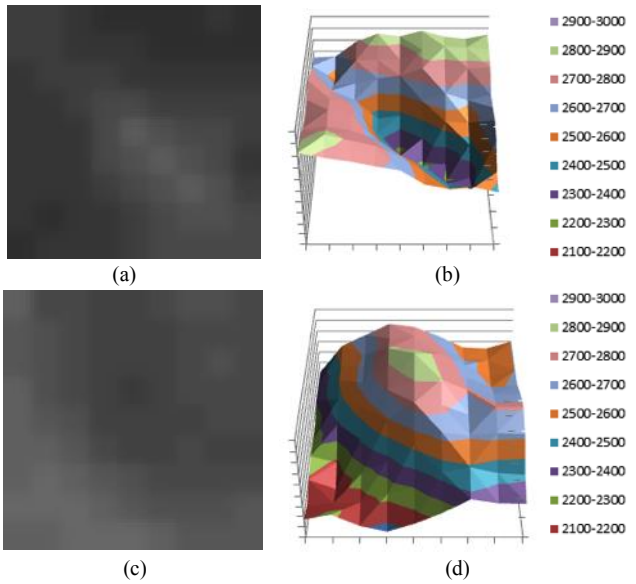

Figure 4. Examples of ROIs with/ without linear structures. (a) Original image with linear structures. (b) 3-D space where the z-axis is the density of (a). The direction of (a) is defined as 135 degree because the output value calculated with the direction filter shown in Fig. 3 (a7) is the smallest value among 16 values calculated using eight direction filters and eight background filters. (c) Original image without linear structures. (d) 3-D space where the z-axis is the density of (c). The direction of (c) is not defined because the output value calculated with the background filter shown in Figure 3 (b6) is the smallest value among 16 values calculated using eight direction filters and eight background filters.

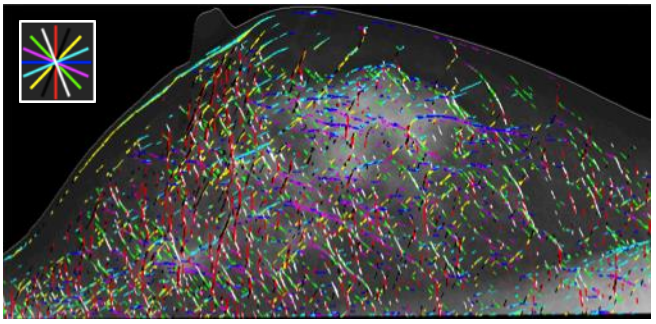

Figure 5. Example of linear structures extracted using our new method. Eight colors represent the directions in each ROI defined by direction filters.

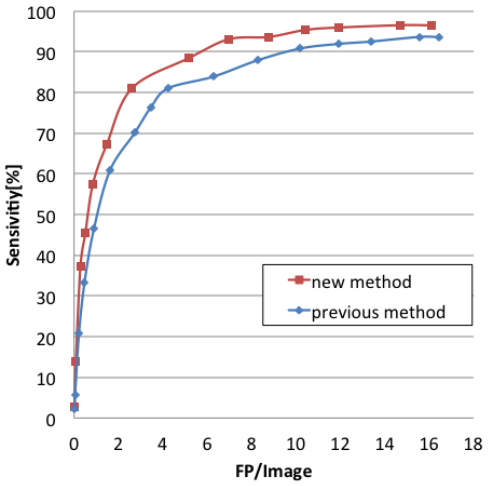

Figure 6. Free-response receiver operating characteristic (FROC) curves of our previous and new methods.

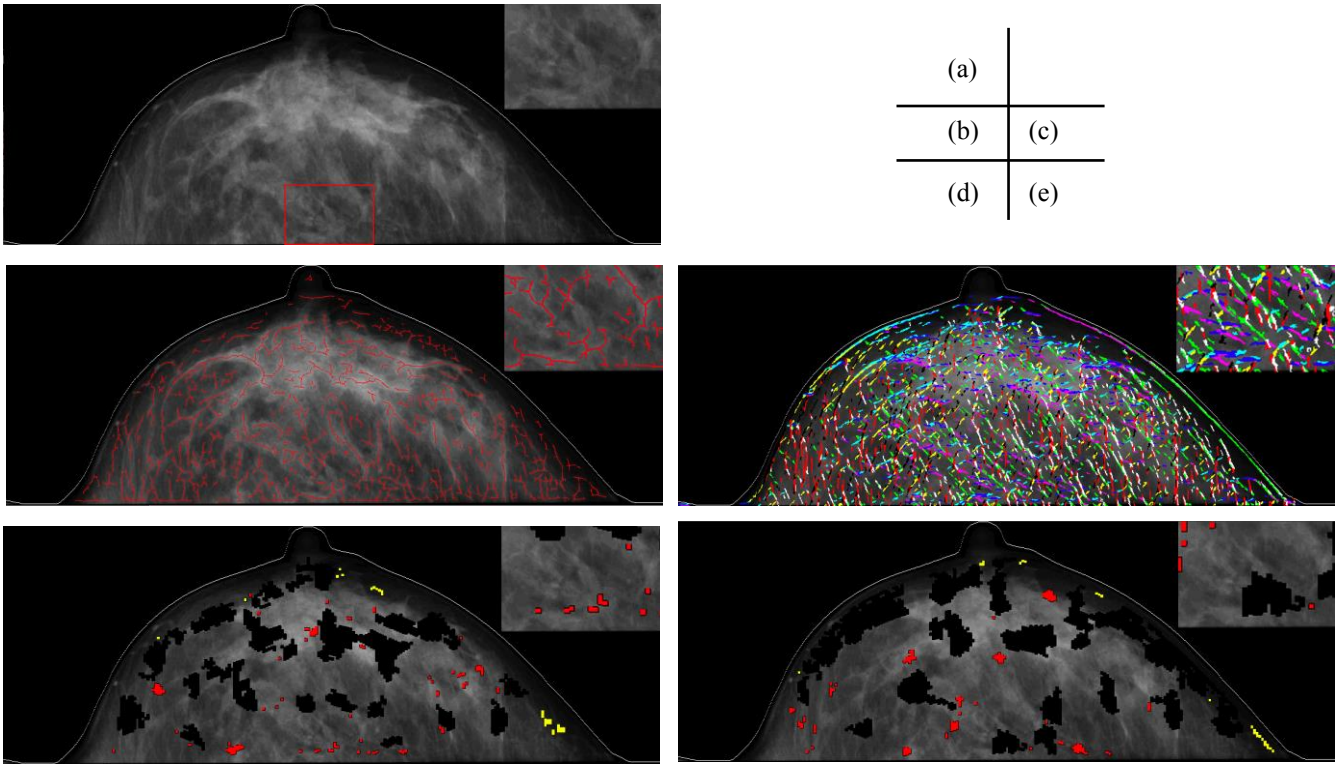

Figure 7. Example of results at the first pick-up stage using our previous and new methods.
(a) Original image with spiculated architectural distortion indicated by a red rectangle. Images (b) and (c) are extracted linear structures using previous and new methods, respectively. Eight colors in (c) show the directions (also shown in Figure 5). It is possible to extract more structures that are possibly related to distorted areas using the new method. (d) and (e) Extracted areas using the previous and new methods, respectively. Red indicates FP areas eliminated because of small size. Yellow indicates FP areas eliminated because of small size and pixel value. Black indicates candidate area at the first pick-up stage. Although the distorted area is eliminated using the previous method, it is extracted using the new method. Each image on the upper right of (a), (b), (c), (d) and (e) is an enlarged image within the red rectangle in (a).

and new methods, respectively. It is expected that the number of FPs per image can be decreased by investigating the difference between extracted FP areas using the previous and new methods and revising the FP elimination step according to the FP method used in the first pick-up stage in the new method.

Figure 7 shows an example of the result at the first the pick-up stage using the previous and new methods. Using the previous method, the distorted area is eliminated at the FP elimination technique stage because of the small size. However, this area is extracted using the new method because the extraction performance for linear structures is improved using the linear direction analysis.

IV. CONCLUSIONS

We propose a new automated method for direction analysis of linear structures to improve the detection of spiculated architectural distortions in mammograms. The FROC curves demonstrate that the results of the new method are superior to those of the previous method. This shows that our new method is effective for detecting spiculated architectural distortions.

Future studies are warranted, in order to decrease the frequency of FPs to facilitate clinical use of this method.

REFERENCES

[1] D. B. Kopans, Breast imaging. J. B. Lippincott Company, 1989.

[2] H. Burrell, A. Evans, A. Wilson, and S. Pinder, "False-negative breast screening assessment: what lessons can we learn?," *Clin. Radiol.*, vol.56, no.5, pp.385-388, May 2001.

[3] R.E. Bird, T.W. Wallance, and B.C. Yankaskas, "Analysis of cancers missed at screening mammography," *Radiology*, vol.184, no.3, pp.613-617, Sep. 1992.

[4] A. Baker, E. L. Rosen, J. Y. Lo, E. I. Gimenes, R. Walsh, and M. S. Soo, "Computer-aided detection (CAD) in screening Mammography: Sensitivity of commercial CAD systems for detection architectural distortion," *A.J.R.*, vol.181, no.4, pp.1083-1088, Oct. 2003.

[5] Karssemeijer N, Te Brake GM, "Detection of stellate distortions in mammograms," *IEEE Trans Med Imaging*, vol.15, no.5, pp.611-619. 1996.

[6] Q. Guo, J. Shao, and V. Ruiz, "Investigation of support vector machine for the detection of architectural distortion in mammographic images," Journal of Physics: Conference Series, 15, pp.88-94. 2005.

[7] G. D. Tourassi, M. D. David, and C. E. Floyed, "A study on the computerized fractal analysis of architectural distortion in screening mammograms," *Phys. Med. Biol.*, vol.51, no.5, pp.1299-1312, Mar. 2006.

[8] R. M. Rangayyan, S. Banik, J. Chakraborty, S. Mukhopadhyay, and J. E. L. Desautels, "Measures of divergence of oriented patterns for the detection of architectural distortion in prior mammograms," *Int. J. Comput. Assist. Radiol. Surg.*, vol.8, no.4, pp.527-545, Jul. 2013.

[9] R. Yoshikawa, A. Teramoto, T. Matsubara, and H. Fujita, "Automated detection of architectural distortion using improved adaptive Gabor filter," Proc. of IWDM2014, pp.606-611, 2014.

[10] N. Yamada, T. Matsubara, A. Tsunomori, T. Hara, C. Muramatsu, T. Endo, H. Fujita, "Comparison of automated detection performance of architectural distortion on two kinds of mammograms," Proc. of IFMIA2012, article no. 64, 2012.